EMBEDDED SELECTIVE LOAD CONTROL FOR EDGE-DEPLOYABLE UNINTERRUPTIBLE POWER SUPPLY MANAGEMENT WITH MACHINE LEARNING–READY ARCHITECTURE

Fawad Ali[1], Saad Khan[2], Zarwa Sohail[3], Tehreem Zahid[4], Muhammad Amir[5]
Humayun Shahid[*6], Bilal Ur Rehman[7], Kifayat Ullah[8], Feroz Shah[9]

[1,2,3,4,5,7,8]*Department of Electrical Engineering, University of Engineering and Technology, Peshawar, Pakistan*
[*6]*Department of Telecommunication Engineering, University of Engineering and Technology, Taxila, Pakistan*
[9]*Department of Mechanical Engineering, University of Engineering and Technology, Peshawar, Pakistan*

DOI:https://doi.org/10.5281/zenodo.17511915

Keywords
Selective load shedding, Branch-circuit priority control, Machine learning, State-of-charge (SoC) estimation, Edge Computing

Article History
Received: 27 August 2025
Accepted: 18 October 2025
Published: 31 October 2025

Corresponding Author: *
Humayun Shahid

Abstract
Single-phase UPS installations fail in an all-or-nothing manner; even brief overloads or unexpectedly lengthy outages can trip the UPS or cause the batteries to fail, resulting in all circuits shutting off, regardless of the mission-critical nature of the circuits. The paper formalizes and evaluates a low-cost microcontroller-based supervisory controller that monitors mains and UPS voltage, as well as branch-level currents, and operates two sets of relay banks to shed/re-energize branch circuits based on a declared priority tree operating on two-time scales. The first, fast-acting protective layer ensures that overload and over-discharge situations are mitigated. In contrast, the second, slow-restoration layer utilizes battery-aware hysteretic thresholds (calculated at 11.4V ("trim"), 11V ("keep only essentials"), and 10.5V ("protective cutoff"). In Proteus step-stress experiments on three branches with a total capacity of 230V/2kW, operating against a 5.9kW UPS ceiling, the controller will complete the elimination of incipient overload by shedding the lowest-priority active branch while maintaining the highest-priority branch until the final shelf. Once the headroom is sufficient, the restoration process is smooth and non-oscillatory. Beyond these outcomes of empirical rules, architecture and literature review outline the rationale for autonomy-aware control, including embedded feasible state of charge and state of health estimators, such as data-driven and neural approaches. The controller itself is designed to ingest such estimates when they become available. The combined telemetry stack provided by MQTT, for example, provides the necessary observability to facilitate and justify this integration. Therefore, the proposed system converts binary UPS failures into graceful, priority-based degradation, paving a clear course for future machine-learning/AI augmentation without altering the underlying circuit-level actuation model.

INTRODUCTION
Lengthy grid outages and brownouts are still common in many regions of the world, and households, clinics, and small businesses in these areas typically use single-phase UPSs for ride-through. In practice, UPS as deployed conventionally has a very "binary" failure mode: a failure longer than anticipated or a transient demand that briefly exceeds the rating of the

inverter will trip on overload or the battery will "give up," leaving all circuits without power, even though only a subset (e.g., refrigeration, lighting, comms) were mission critical. Industry vendors have clearly defined load shedding, which is the process of shutting down crucial non-essential loads in a specific order to extend UPS battery life and save critical functions. However, most small installations still implement this approach in an ad hoc manner and reactively, if at all [1]. This paper is based on the prototype reported in the attached thesis: a microcontroller-based controller that measures UPS/mains voltage and per-branch current, and fires relay banks to shed or focus branch circuits in accordance with declared priorities and real-time supply limits. We formulate that design as an abstract control problem, placing it in the context of current literature, and make the case that circuit-level hierarchical battery-aware, priority-based load control provides greater resilience at a comparatively low cost.

Circuit-level prioritisation has already been validated in commercial offers regarding the user experience. For example, the Leviton Smart Load Centre and SPAN Panel feature application-level controls that allow for defining breakers as either essential or non-essential, and when the backup power is on, automatically drop lower-priority circuits to extend their runtime [2] [3]. Similarly, the concept of "critical-load panels" is highlighted by consumer information sources (4) as the conventional approach when backup capacity is more limited, which would make such an approach both intuitive and accepted by the circuit. The controller we investigate aims to replicate this ability in UPS-only houses (with or without PV), but in a dynamic manner - namely, with no static re-wiring, but with the possibility to re-admit loads as headroom recovers. The addition of dynamic priority enforcement compared to static enforcement is minimal in terms of hardware requirements, but significant in terms of operational value.

A first area of related work is in home energy management systems (HEMS), where priority labeling (using tags and demand caps) has been extensively employed. Recent research suggests that encoding appliance priorities and scheduling them against caps or real-time tariffs can reduce costs and minimize peak usage with minimal loss of comfort. Yang et al. present a dynamic load-priority scheduling scheme that bounds aggregate appliance power during the peak period while maintaining utility, and report significant savings with low computational overhead [5]. Panda et al. further expand this concept with a meta-heuristic adaptive Salp Swarm Optimizer for Priority-Aware Residential EMS, integrated with Renewables, again showing peak shaving and cost improvements [6]. Kanakadhurga et al. propose a MILP-based smart-home EMS jointly optimizing PV, battery, and EV flexibility under the influence of real-time pricing [7].

Furthermore, Apaydink-Ozkan et al. demonstrate that appliance-level scheduling may fulfill user comfort windows without creating peaks [8]. The context of our UPS is different (decisions must be made instantaneously, with actions often irreversible in the short term). However, the central insight carries over: priority labels can be used as an effective proxy for user utility, and should be made first-class control primitives.

A second stream is derived from microgrid resilience, particularly in cases involving under-frequency load shedding (UFLS) and hierarchical restoration. Recently, Wang et al. proposed a two-stage UFLS, in which a fast protective shield guards against frequency decline and a risk-aware stage determines which loads are still to be curtailed to facilitate a principled analysis that separates urgent actions from measured recovery [9]. Surveying UFLS schemes, including the rule-based strategies, adaptive strategies, clustering/ML-assisted strategies, the trend toward context-based shedding, and staged restoration is highlighted [10]. Broader reviews of microgrids focus on hierarchical control, where rapid stability loops ensure safety margins, while slower layers balance economics and comfort [11]. Although a household UPS is not a microgrid in the classical sense, its architecture is similar: a fast protective layer protects the limits of the inverters/batteries (to prevent them from tripping and becoming over-discharged), and a slow restorative layer re-admits non-critical circuits when the margins are restored. We use this separation into timescales as the organising principle of our controller.

A third pillar is awareness of the battery. Some consumer UPSs still use a terminal-voltage threshold to determine when to trip; however, this is a poor indicator of remaining energy, as it is a function of internal resistance, temperature, and recent current history, particularly under a dynamic load. Embedded-feasible state-of-charge (SoC) and state-of-health (SoH) estimation enables more accurate staged shedding and restoration. Bolsi et al. present an adaptive low model NPS for lead-acid batteries, which is an autonomy estimator tailored for UPS using an adaptive Thevenin model [12]. Shang et al. have demonstrated that using the features related to the Coup-de-Fouet phenomenon may give predictive power for VRLA SoH in UPS duty [13]. Fan et al. suggest a non-intrusive SOH estimator based on the dynamical response to load fluctuations - an attractive alternative for embedded controllers that does not allow destructive tests (14). Recent reviews combine model-based, data-driven, and hybrid SoC/SoH techniques, discussing the trade-offs in their deployment [15]. In our design, SoC/SoH estimations are used to feed back hysteretic bands, reserving energy in top-priority circuits, aggressively shedding reserves when a floor is breached, and orderly recovering margin to prevent control chatter.

Implementation details do make a difference when referring to measurement and actuation. Galvanic isolation is required for mains sensing; empirical measurements are provided to document the waveform distortion caused by different resistance transformer-based modules (or isolation circuits) and their impact on RMS and real power calculations in [16]. For per-branch metering, current transducer selection options (open-loop Hall, closed-loop Hall, shunt with isolation, and fluxgate) are a trade-off among cost, bandwidth, and accuracy; recent reviews offer selection criteria for embedded power electronics [17]. On the telemetry side, the MQTT standard is widely used by both energy monitors and prototypes of UPSs as a lightweight publish/subscribe protocol for locally-assisted dashboards and notification [18], [19]. Our controller features the following patterns: transformer-isolated AC voltage sensing, appropriately rated Hall sensors for branch current, a Relay/contactor bank for actuation, and local MQTT telemetry for observability.

We formulate the UPS management problem as follows. Given (i) an inverter with fixed apparent power rating S_{\max } and a short time overload characteristic, (ii) a battery with uncertain SoC/SoH and non linear voltage - SoC behaviour, (iii) a set of branch circuits, labelled based on priority tiers (e.g., P1/P2/P3), and (iv) on line measurements of the mains/UPS voltage and per branch currents design a hierarchical controller that (a) avoids overload trips and over discharge, (b) maximizes uptime of P1 circuits, and (c) restores P2/P3 circuits as soon "Fast" logic imposes guardrails on apparent power and battery protection "slow" logic employs SoC-aware thresholds with hysteresis in shedding/restoration by priority (optionally modulated by user policy, e.g. "keep refrigeration and router on until 20 percent SoC; lighting until 40 percent.")

This paper extends the two-timescale control policy from UPS-only homes to homes with fusing protective guardrails and with priority-aware restoration. Additionally, a battery-aware decision layer is introduced, replacing the crude voltage cut-off with SoC/SoH-aware bands based on an embedded feasible estimation [12]-[15]. Finally, a sensing/actuation concept (isolated voltage measurement, branch-by-branch current metering, and MQTT telemetry) is presented, which aligns with recent evaluations and best practices [16]-[19].

Significance. In outage-prone environments, the marginal value of holding a few circuits alive is enormous: the safe storage of food, lighting, connectivity, and limited medical or IT equipment. Selective continuity using priority-based shedding has been shown in emerging smart panels and in the industry to prolong the autonomy and minimize nuisance outages [1]-[4]. In the case of UPS-only, the strong conceptual framework from HEMS and microgrid research in general (priority as proxy for utility; hierarchical shedding/restoration) and the necessary tools (SoC/SoH estimation; safe sensing) can be used to develop a reliable controller. The rest of the paper reviews these strands, identifies gaps that our approach spans, and then introduces the architecture and evaluation.

LITERATURE REVIEW

Literature has evolved from static day-ahead scheduling with time-of-use pricing schemes to dynamic, priority-sensitive approaches. Yang et al. propose a dynamic load-priority approach to restrict the aggregate appliance load and maintain service quality during peak periods, with a low computational burden and tangible savings, for simulations calibrated with residential dwellers' usage patterns [5]. Panda et al. develop an adaptive Salp Swarm heuristic that considers photovoltaic generation and storage. Their controller, by explicitly encoding appliance priorities, can improve both peak shaving and energy cost compared to baseline heuristics [6]. Kanakadhurga and Prabaharan's MILP-based energy management system optimizes electric vehicle flexibility with PV-battery operation under real-time pricing. The main point is that priority and flexibility need to be co-optimized to keep bills as low as possible without contravening the user's constraints.13, 7 Other complementary studies, such as Apaydin-Ozkan et al. 's comfort-respecting scheduler, show that the comfort-cost conflict can be controlled by dividing appliances into priority and controllability classes [8]. Taken in combination, these works support the use of priority tags as concisely and powerfully defining descriptions of user utility; therefore, they are natural inputs to any controller that must shed loads in situations where supply is constrained (representative sources [5]-[8]).

Typically, HEM studies make assumptions about schedulable appliances (e.g., dishwashers) and forecast horizons of hours to a day. A UPS controller, on the other hand, is impoverished in several ways: Outages come and go with little notice, inverter saturation is hard to control, and control must be exercised at circuit granularity (with line cycle-to-second response times). In addition, however, the proper abstraction remains a priority. Already in the market, there exist products (Leviton, SPAN) that offer labels for essential versus non-essential circuits and automatically shed when using backup power [2] - [4]. Our controller implements this concept for online UPS-only systems, providing critical load backup continuity through real-time circuit prioritization, rather than a fixed set of subpanels or manual switches.

Load shedding is considered a first-class control action in system protection research for stability purposes. In this paper, we adapt the two-stage under-frequency load shedding (UFLS) scheme for microgroups of Wang et al. [9], which is characterised by a fast operation to prevent instability (grid-scale frequency collapse; UPS-scale inverter overload or DC undervolting), followed by a slower optimisation to determine which loads to turn off and on. Skrjanc et al. [10] identified UFLS designs in their systematic review, which include rule-based, adaptive, and clustering-based designs. There has been a shift towards context-aware restoration, considering risks and priorities, not just megawatts. Microgrid studies also further confirm the conventional adoption of hierarchical management as the default, in which stability assurance is decoupled from secondary and tertiary objectives [11]. The algorithm is mapped one-to-one to UPS, yet it is poorly explored in the literature: fast guardrails are enabled, and battery protection is implemented. A slower priority-band hysteresis is used for restoration as the state of charge and power headroom improve. Our contribution is to realize such a mapping at the household scale using low-cost sensing and actuation.

Related distribution-level studies consider dynamic shedding and restoration using synchrophasors and wide-area control. However, the sensors differ, the supervisory logic (responding immediately to prevent collapse, and then restoring cautiously) remains the same [20]. For UPS-only applications, it is sufficient to place the super-sensory layer on top of protection trips to transform immediate total blackouts into graceful degradation: P1 circuits stay in, while

P2/P3 are tripped and brought back depending on the remaining margin.

Any scheme that attempts to undermine autonomy needs to consider the state of the energy store. Terminal voltage thresholds, which are still used in consumer UPSs, are not load-accurate. Bolsi, S, Sassone, L., & Catalini, G. (2017). A UPS-specific autonomy estimator for lead-acid battery based on an adaptive equivalent circuit model: Improved remaining life prediction under actual discharge profiles. [12] Shang et al. utilize the coup de fouet nadir to interpret the VRLA state of health in backup events, allowing life-protective decisions to be made without invasive testing [13]. Fan et al. employ a non-intrusive method for predicting the state of health based on voltage system responses to load surges and wavelet-derived features with a neural estimator, demonstrating great potential for use in embedded controllers that are unable to carry out deep characterization [14]. Kunatsa et al. Comparison of approaches for state-of-charge estimation in storage technologies: observers (e.g., EKF/UKF), data-driven regression, and hybrid methods, and the role of robustness with respect to temperature and ageing [15]. We draw two conclusions. First, even lightweight estimators are superior to voltage thresholds for determining whether to shed or restore low-priority circuits. Second, the controller must be chemistry-agnostic (VRLA vs. Li-ion): it takes SoC/SOH estimates from whatever battery management system/estimator is available. It applies hysteretic policy bands to reserve energy for P1 circuits and prevent oscillation near limits (these sources [12]-[15]).

Accurate measurement at mains potential with safety.: Accurate and safe measurement is fundamental to any closed-loop controller operating at mains potential. Havrlik et al. measure the distortion added by galvanic-isolation methods (e.g., small potential transformers, optocoupler-based circuits) and their impact on active-power estimation, providing a helpful guideline for selecting and calibrating voltage-sensing equipment for residential panels [16]. For current measurement, recent reviews combine the trade-off space of current transducers in open- versus closed-loop Hall sensors, shunts, and fluxgate devices to map accuracy, bandwidth, cost, and safety isolation to specific use-case applications [17]. Regarding communications, MQTT is very popular in embedded monitors, such as UPS-oriented prototypes. Because publish/subscribe messaging reduces network and CPU overhead, it allows for local dashboards (e.g., Node-RED) [18], [19]. We make the corresponding design decisions for our implementation, including transformer isolated voltage measurement, breaker-rated Hall sensors per branch, and MQTT telemetry, to make the system's status (on/off, state-of-charge estimate, headroom) transparent without any cloud dependencies.

User-Facing Products Support the Value Proposition of Circuit-Level Priority Control on Backup Power. Leviton's published materials emphasize the ability of users to assign essential circuits versus non-essential circuits, and that the system can automatically shed non-essential loads in the event of a grid failure when integrated with an automatic transfer switch [... 2]. The panel and app implemented by SPAN employ three-level priorities for backup (must-have, nice-to-have, not essential) and present real-time runtime projections (i.e., the consumer equivalent of our priority bands and autonomy estimations) [3], [4]. While these solutions are usually geared towards at-home batteries or generators, the usage model—prioritizing continuity where it counts—translates readily to UPS-only homes.

Despite the presence of strong streams in HEMS, microgrid shedding, and battery estimation, we found limited peer-reviewed treatments that specifically address UPS-only homes at branch-circuited granularity, assuming no photovoltaic generation, whole-home batteries, or utility-coordinated demand response. Although vendor FAQs, product pages, and prosumer resources recognize the potential of priority-based shedding to extend autonomy [1]-[4], the academic optimization and control literature relatively seldom explicitly deals with the coarse controllability (whole circuits), strict real-time limitations, and hard limits of small UPSs. This paper contributes in the form of a two-timescale controller that (i) UFLS-style hierarchy is introduced to the UPS domain [9]-11, (ii) state-of-charge/state-of-health-aware thresholds are introduced using the design of embedded-feasible estimators [12]-15, and (iii) a measurement/telemetry stack is specified that is consistent with safety and cost limits [16]-19. The resulting solution is a blueprint that transforms typical UPS deployments from "all-or-nothing" to graceful degradation, coupled with speedy restoration, all based on the same priorities that users already know, thanks to smart panels.

DESIGN METHODOLOGY

This methodology implements and evaluates a priority-based UPS load management controller through a simulation-focused workflow in Proteus. The approach begins with a system-level architecture, which breaks the problem into sensing, decision, and actuation blocks. After. After mapping these blocks to actual circuits and modules, the integrated model is exercised under the design parameters set for loads and the UPS. The primary approach, based on the literature review, is to model user intent as circuit-level priorities and to achieve a two-timescale policy that makes fast protective decisions and slower restorative decisions. The battery reserve awareness is used to determine when and how loads are shed or restored. The high-level diagram is in the form of a block diagram that lists alternating-current voltage measurement, alternating-current current measurement, direct-current voltage measurement, a microcontroller unit, and switching relays. This view serves as the basis for all subsequent implementation decisions, as shown in Figure 01.

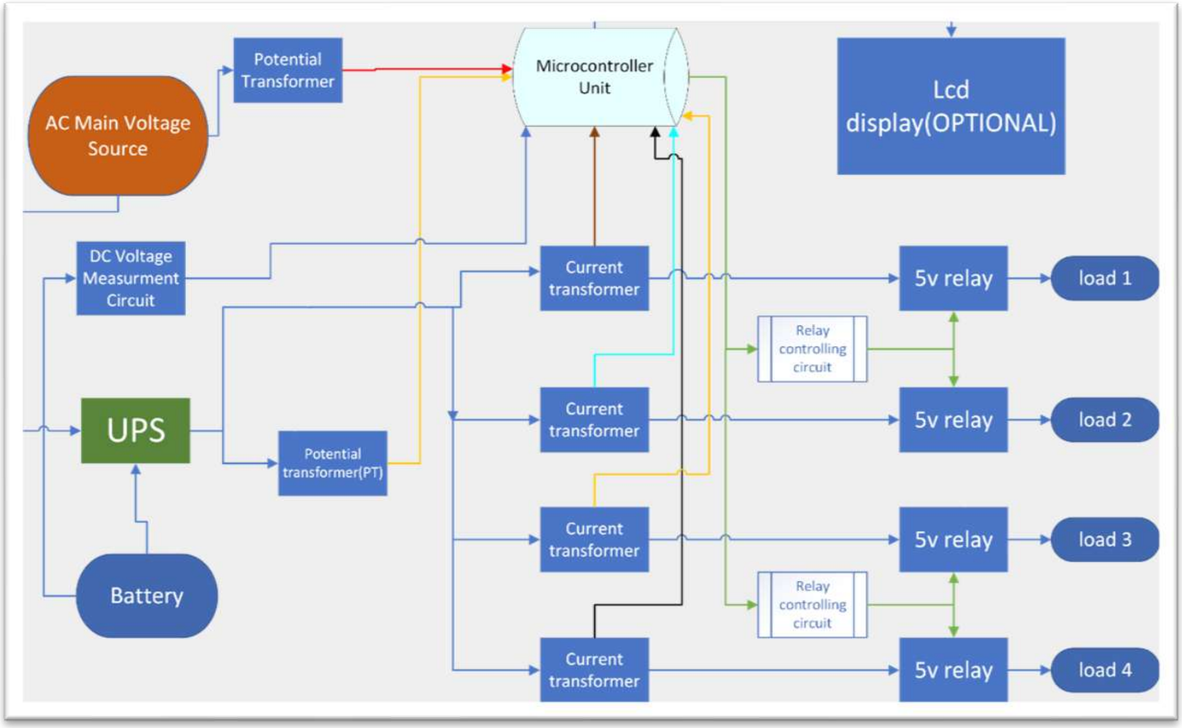

Figure 01: System-level block diagram detailing the architectural insights

As far as the testbed configuration and simulation parameters are concerned, the setup was parameterized with (i) a three-branch load set and (ii) a single-phase UPS. The load set depicted in Table 01 comprises three 230 V branches, each specified with operating voltage and current/power values used to initialize the branch models.

No.	Label	Operating Voltage (V)	Current Consumed (A)	Power (W)
1	Load 1	230	8.6	2000
2	Load 2	230	8.6	2000
3	Load 3	230	8.6	2000

Table 01: Overview of connected loads and their specifications

Likewise, the uninterrupted power supply specification, detailed in Table 02, provide input/output voltages and total capacity, which we use as the apparent-power ceiling for protective logic and headroom computation.

Input AC Voltage (V)	Input DC Voltage (V)	Output AC Voltage (V)	Output DC Voltage (V)	Total Capacity (KW)
230	14.2	230	14.2	5.9

Table 02: Specifications and Performance Characteristics of the Uninterruptible Power Supply System

The mains alternating-current voltage is sampled by a special measurement system, which reduces the high line potential to an analog value that is safe for acquisition by the controller. This conditioning is necessary not only for electrical protection and suitability for the low-voltage input channels, but also, as it maintains the waveform's shape fidelity, it permits the controller to read downstream signals accurately.
The resulting voltage channel serves as the basic reference against which all currents of the load are checked to determine the actual power consumption and enforce the branch limits with precision by the controller.
Moreover, this same voltage channel is continuously monitored to detect abnormalities at the source, such as under-voltage, over-voltage, or complete mains power loss, which can then trigger action necessary to protect or switch it off.
The complete implementation of this function is illustrated in the primary voltage measurement schematic of Figure 02, with an emphasis on both the scaling components and the isolation features required to ensure safe and reliable operation.

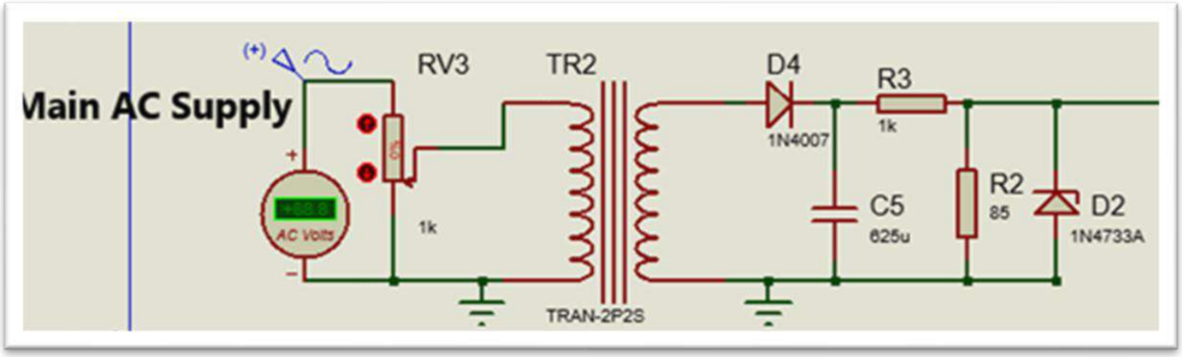

Figure 2: System-level block diagram of the architectural insights.

The output of the UPS is also connected to a separate measurement path, allowing the controller to continuously measure the voltage and verify control validity during islanded operation, as well as to ensure control validity after a transfer. This arrangement is shown in the uninterruptible power supply (UPS) output voltage measurement schematic, which is highlighted in Figure 03.

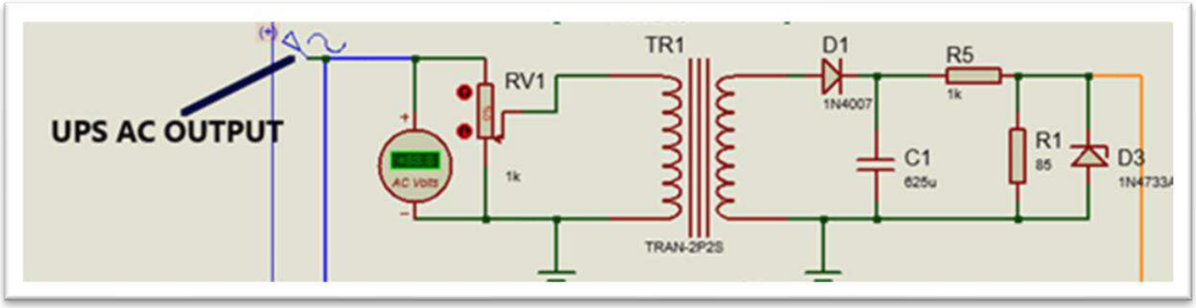

Figure 03: System-level block diagram detailing the architectural insights

Together with random sequence detection, the dual measurements form the basis for continuous source change adaptation and provide the quantitative basis for real-time apparent power estimation implemented in the firmware logic, which is consistent with the requirement for stable sensing in changing operation modes, as outlined in the literature. In the case of the Proteus model, both channels are tied to dedicated analog inputs on the controller, and the scaling factors and reference points of the channels are described in the schematics for easy verification prior to running each simulation.

Branch-specific load monitoring is accomplished using a Hall-effect current sensor, as referenced in the material, which is the ACS712 integrated circuit. This device upconverts the branch current to a low-voltage analog signal, which is sampled by the controller, enabling it to make decisions consistent with user priorities at a circuit granularity. The accompanying figure illustrates the role of this device in the model, serving as a reminder that calibration and orientation will be crucial in hardware implementation. The simulation reflects the expected polarity and nominal sensitivity, as shown in Figure 04.

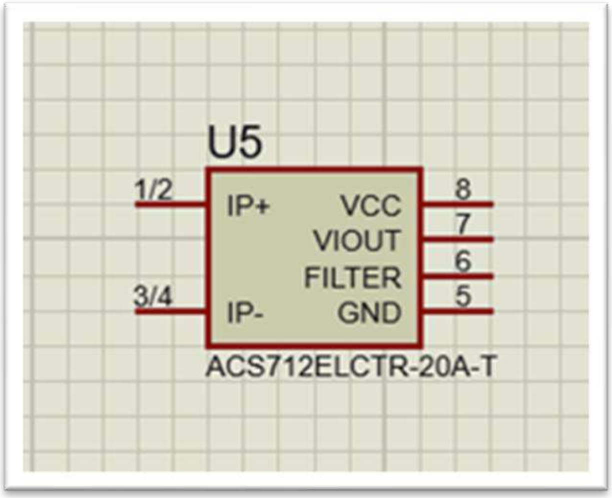

Figure 04: ACS712ELCTR-20A current measurement IC

The controller also monitors the direct current bus of the battery power supply from the UPS to track the reserve. This is achieved through the DC-voltage measurement circuit, which forms the basis for the reserve band, as shown in the simulation. The circuit used for pro,gasmming systematic load shedding and restoration is illustrated in Figure 5 of the chapter figure set. The measurement paths used for the network schematics are actually drawn in such a way that during bench validation, the exact pin mapping can be replicated without ambiguity.

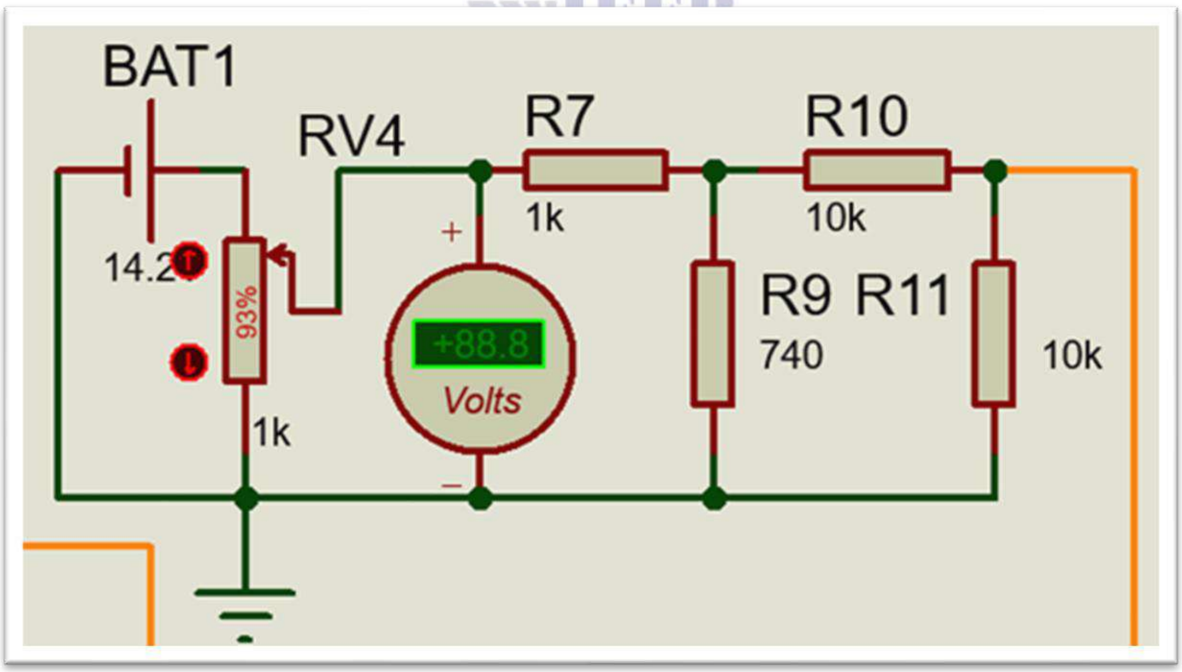

Figure 05: Battery DC voltage measurement circuit

To drive mains-rated switching hardware from low-level microcontroller outputs, the design includes a driver stage consisting of a transistor array, as shown in the ULN2003A integrated circuit data sheet. This block ensures that logical command impulses can drive relay coils within their electrical limits, with the amount of noise immunity consistent with the needs of the electromechanical interface, as shown in Figure 06.

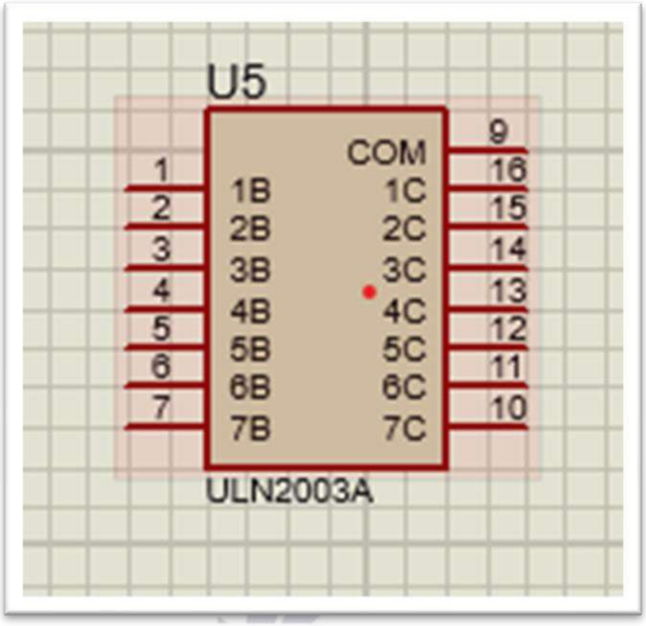

Figure 06: ULN2003A IC

Power switching is achieved by relays specifically designed for 12-volt coil excitation, and contact specifications have been selected in accordance with the simulated branch loads. The accompanying schematic, featured in the Figure, exhibits standardized wiring conventions. Additionally, contact logic is marked for both simulating fidelity and facilitating after-hardware implementation. In line with the robust and interpretable treatment of interventions in the prevailing literature, the controller switches off, in turn, the circuit with the lowest priority during periods of reduced capacity or low reserve levels, and switches on the circuits in the same order during periods of increased capacity and reserve. Proteus-created relays are positioned in series across each branch of the entire schematic, allowing for instantaneous visual checking of the circuit conditions throughout the execution of each scenario.

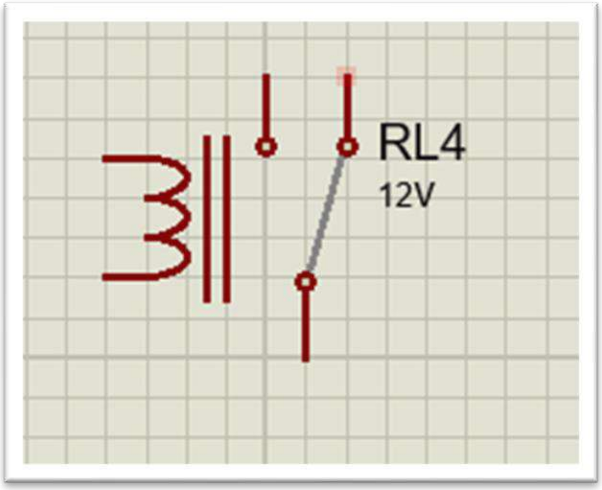

Figure 07: Volt Relay Schematics

Operator awareness and rudimentary explainability are illustrated by a character liquid crystal display, as shown through a four-line interface schematic. This display shows real-time measurements and the actual admission set during experiments, making the progression of control actions visible in the same instrumentation view that a field user would see, as shown in Figure 08.

Figure 01: 16x4 LCD Display Schematics

The computational part of the system is implemented on an Arduino Mega 2560 microcontroller, chosen for its large number of available analog input channels and the numerous general-purpose input/output (I/O) pins it offers.

These features make the platform especially suitable for applications where multiple acquisition of sensor signals and simultaneous control device actuation is required.

The modeling of the board is performed directly in the Proteus environment, allowing for the simulation and verification of the hardware/software interactions before the hardware is physically deployed.

The corresponding schematic clearly shows the mapping of each sensor channel to its corresponding analog input pin. This makes the flow of signals really clear and makes future troubleshooting/expansion really easy.

Additionally, the design confirms that all control lines are correctly connected to the relay drive circuitry, which in turn connects the logic-level outputs of the microcontroller to the higher-amplitude switching elements required for branch control.

This integration is illustrated in Fig. 9, which provides an overall view of the computational unit as the master orchestrator between sensing and actuation.

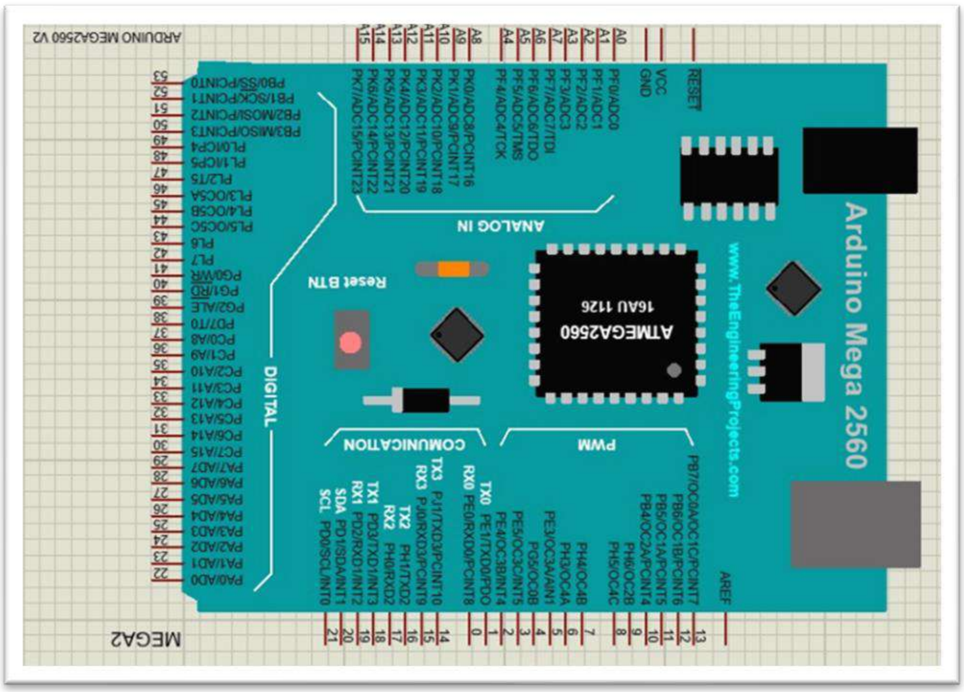

Figure 09: Arduino Mega 2560 Proteus Schematics

Ultimately, the entire plant and control assembly are represented by an integrated schematic to the extent that it is possible to trace the order of execution, wiring, and signal flow from any measurement point to the associated control decisions. This diagram of the top level serves as the canonical reference for both simulation replication and bench build translation, as shown in Figure 10.

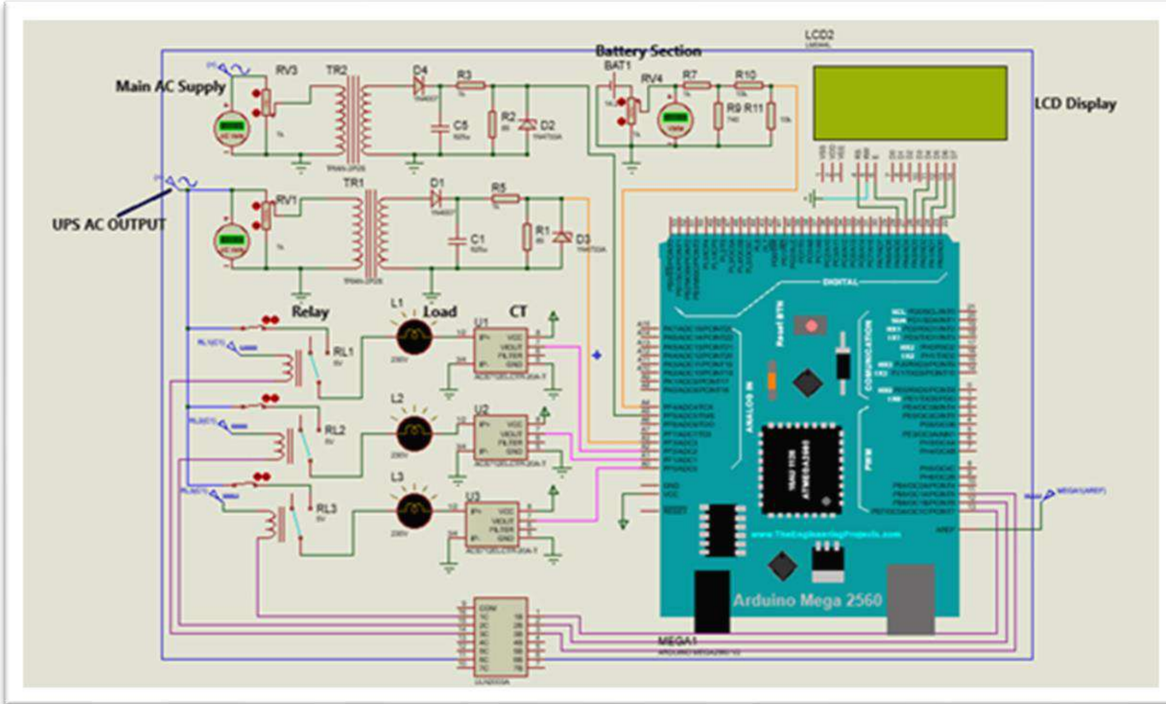

Figure 10: Arduino Mega 2560 Proteus Schematics

The integrated diagram serves as a procedural checklist before every experimental run, ensuring that the proper power rail settings, reference connections, and default relay state are in place. With the architectural structure decided, an explicit design for the loads and uninterruptible power supply is planned in the simulation plan. Three branch loads are specified, each operating at 230V, 2000W, hence giving different stepwise variations in demand as branches are integrated or removed. The. The accompanying table in the chapter documents the labels, Operating Voltage, Current, and Power for these branches. The uninterruptible power supply specification specifies both alternating and direct input and output voltages. It provides a total capacity of 5.9 kW, which serves as the upper limit for the experiments to prevent overload of the supply logic. This confluence of defined loads and one capacity constraint enables (unambiguous) controller testing in progressive stress and recovery sequences, representing an emphasis found in the literature on circuit-level-based decision making as opposed to individual appliance scheduling. Prior to each scenario, the figures and tables are cross-checked across the model to ensure that the numerical values provided in the tables reflect the scaling present in the sensor in the schematics.

Moving on, the design methodology describes the assembly of each sensing and actuation block in the model and explains the microcontroller's consumption of these channels. Alternating-current voltage measurement is carried out by a potential transformer, which reduces the voltage in the line to a safe level. Alternating-current current measurement is accomplished by multiple current transformers that provide proportional indications of the various branch conductors, and both of these feed the analog inputs of the controller. Direct current voltage measurement is observed at the battery side of the uninterruptible power supply, serving as a reserve proxy for energy-aware control in the simulation. The microcontroller processes these inputs, applies pre-programmed logic, and can actuate the relay drivers to connect or disconnect loads. Each of these functions is clearly expressed in the methodology section of the chapter, closing the circle from sensing to action in a way that resembles the call for priority-encoded, hierarchical control with reserve awareness as expressed in the review of the literature. To aid reproducibility, the wiring conventions and pin allocations, as shown in the device figures, are maintained in the complete Proteus schematic to ensure that every signal path can be interrogated with virtual instruments when running, without the need to modify the control program.

RESULTS

The simulation campaign demonstrates that the proposed microcontroller-based controller achieves selective continuity in real-life operating conditions within the Proteus environment. With a 230 V mains supply available, the controller is used to energize all user-enabled circuits and to constantly display measurements on the LCD, thus establishing the baseline for subsequent comparisons and validating proper sensing and actuation in steady state, as shown in Figure 11.

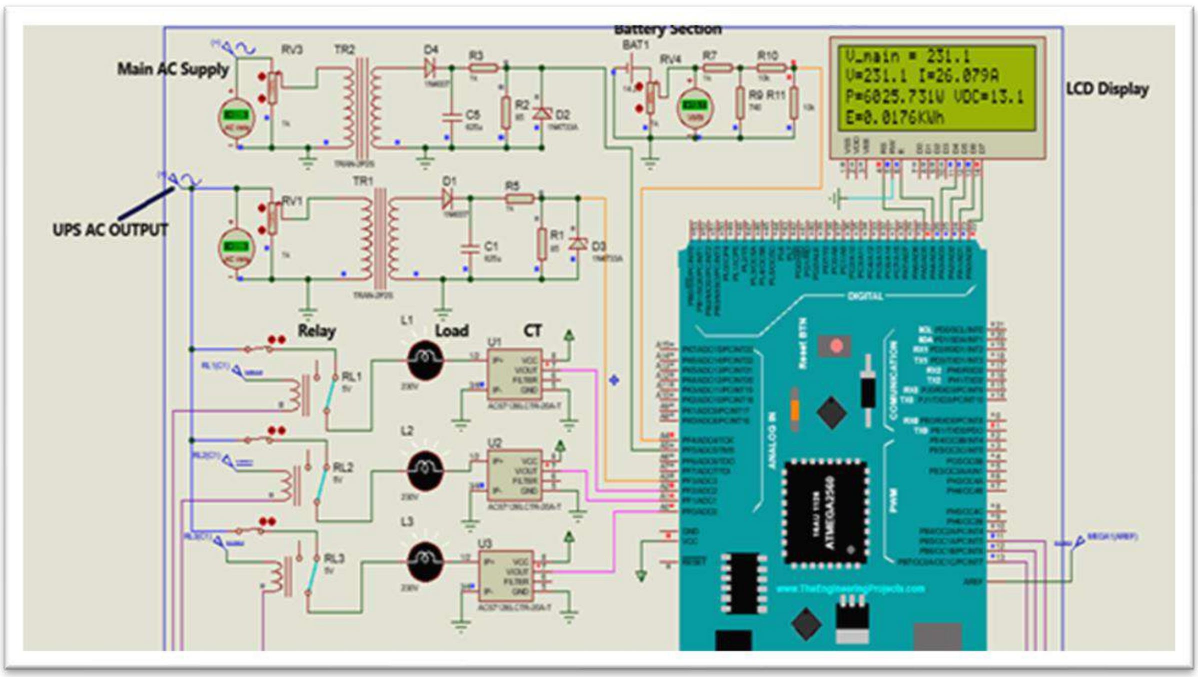

Figure 11: Proteus schematic representation of a standard 230V main power supply circuit

Upon the loss of mains as shown in Figure B, the system switches without interruption to UPS mode, maintaining the same load management priority rules. This operational sequence empirically validates the accurate detection of the power outage event and the appropriate deployment of the UPS as a source of alternative energy, providing uninterrupted service to the activated loads in compliance with the power ratings specified and demonstrated in Figure 12.

In both operational scenarios — i.e., under normal mains-connected conditions and during UPS-supported backup — the liquid crystal display (LCD) interface is the primary observability mechanism for the simulation operators. It provides real-time and immediate feedback on the system's state transition and quantitatively evaluates relevant electrical parameters..

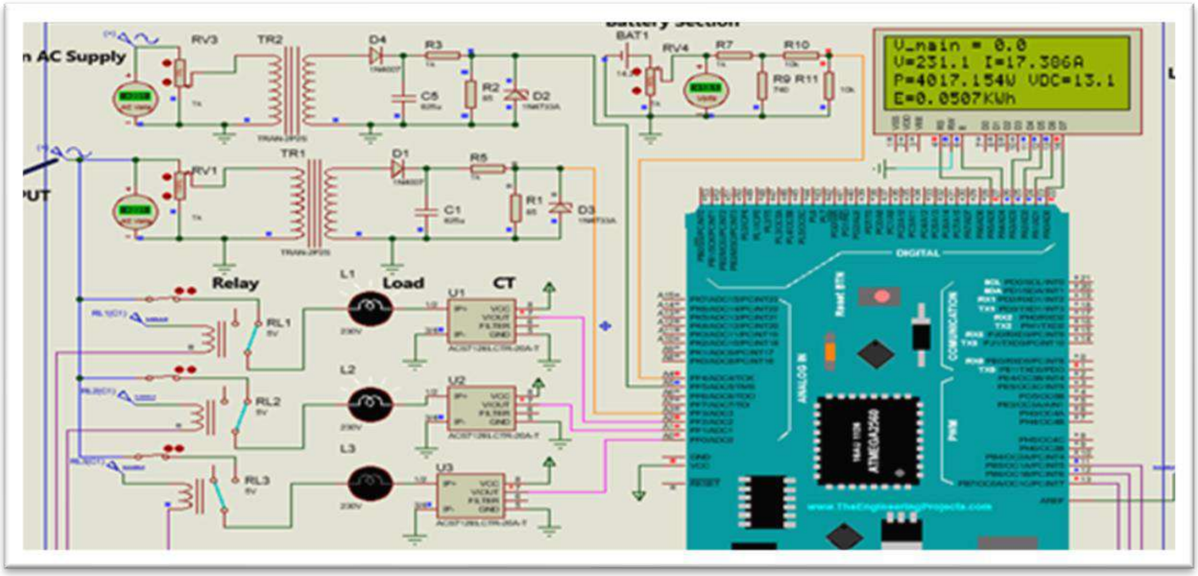

Figure 12: Proteus schematic representation of a standard 230V main power supply circuit

A progressive-stress test, also known as a load-increasing experiment, is used to test the protective layer of the policy, independently of the battery thresholds. The model uses three nominally identical branches at 230 V and 2000 W power rating, per branch, which helps establish clear "binary" steps at each point where the aggregate apparent power is less than or greater than the UPS rating (there is little ambiguity about whether there is less than or greater than the UPS rating).

When Load 1 is the only admitted load, as shown in Figure 13, the controller perceives enough headroom and therefore maintains the system state as it is.

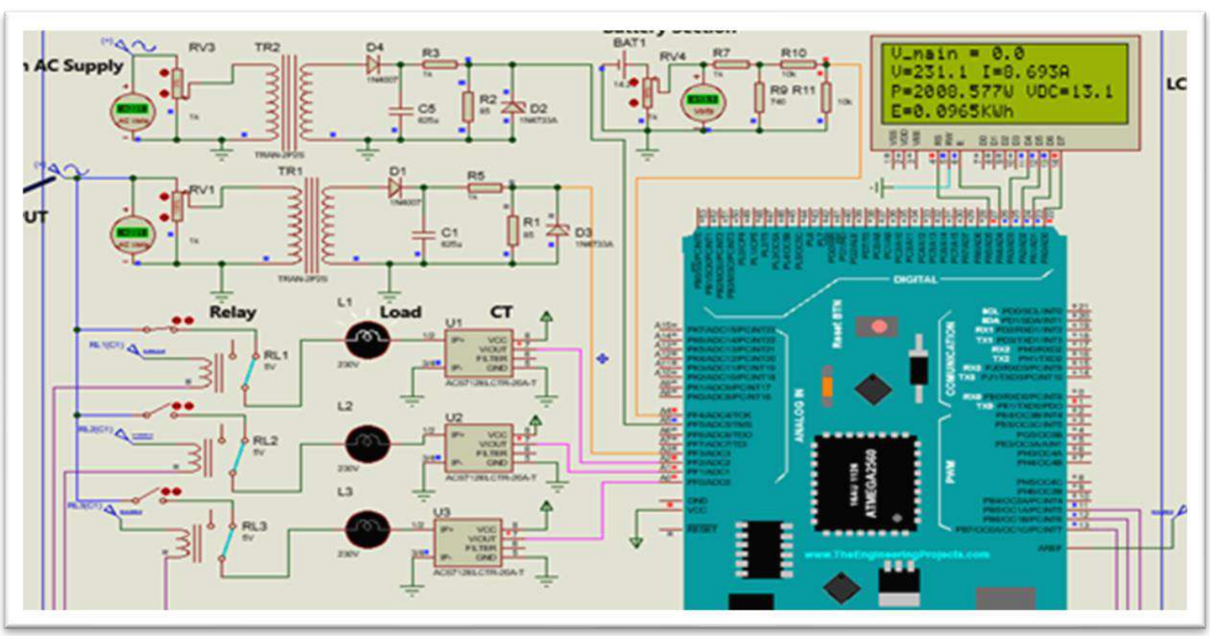

Figure 13: Proteus schematic representation of a standard 230V main power supply circuit

Also, when Load 2 is also admitted, total demand is still under the UPS capacity and both remain on, as per schematic detailed in Figure 14.

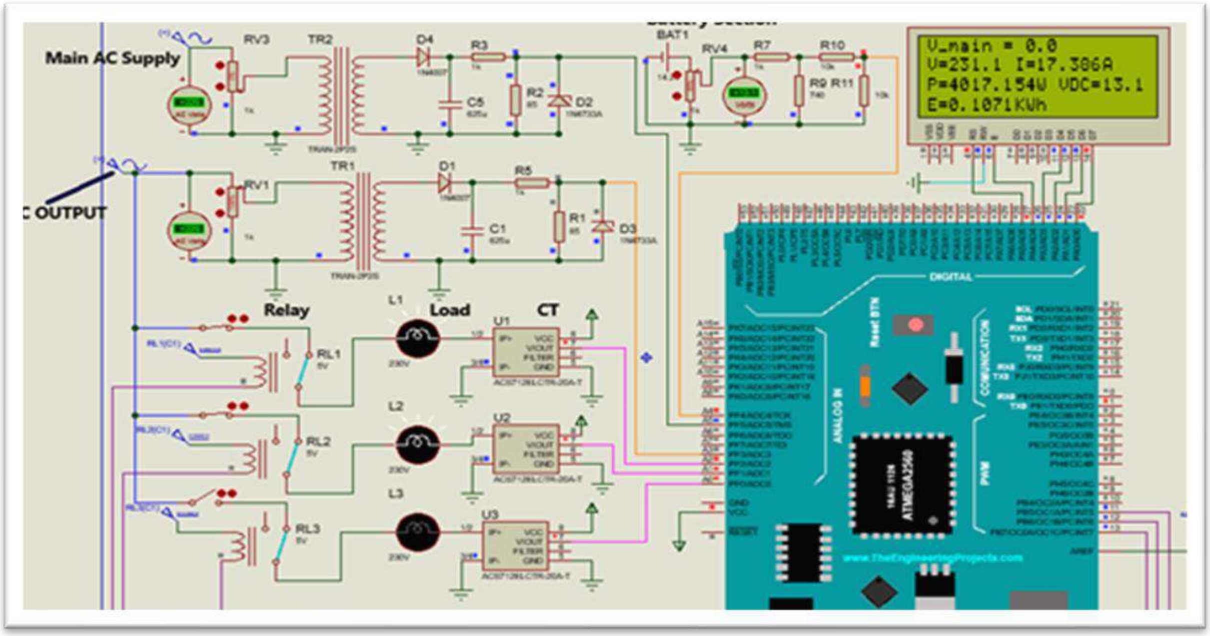

Figure 14: Detailed proteus schematic diagram illustrating the configuration and integration of Load 2 within the electrical circuit

In the event that an attempt is made to incorporate Load 3 into the operational electrical circuit, the cumulative power demand surpasses the predefined capacity threshold established for the system, thereby posing a risk of exceeding the system's rated operational limits. In response to this overcapacity condition, the system's controller, operating in strict accordance with its preprogrammed decision-making logic, initiates a protective mechanism designed to mitigate the risk of overload. Specifically, the controller identifies and deactivates the branch assigned the lowest priority within the load hierarchy, which, in the context of this particular system architecture, corresponds to the newly integrated branch, namely Load 3.

This deliberate and strategic disconnection serves to promptly restore the total aggregate power demand to a value that falls within the system's designated rated capacity, thereby ensuring the preservation of operational stability and preventing the onset of potentially deleterious overload conditions that could compromise system integrity. The entire dynamic load management process, encompassing the prioritization framework, the selective disconnection protocol, and the subsequent stabilization of power demand, is comprehensively depicted in Figure 15. This figure provides a clear visual representation of the system's adaptive response to the overcapacity scenario, illustrating both the triggering of the protective mechanism and the successful restoration of the system to compliance with its specified power constraints, thereby underscoring the efficacy of the controller's load-shedding strategy in maintaining operational reliability.

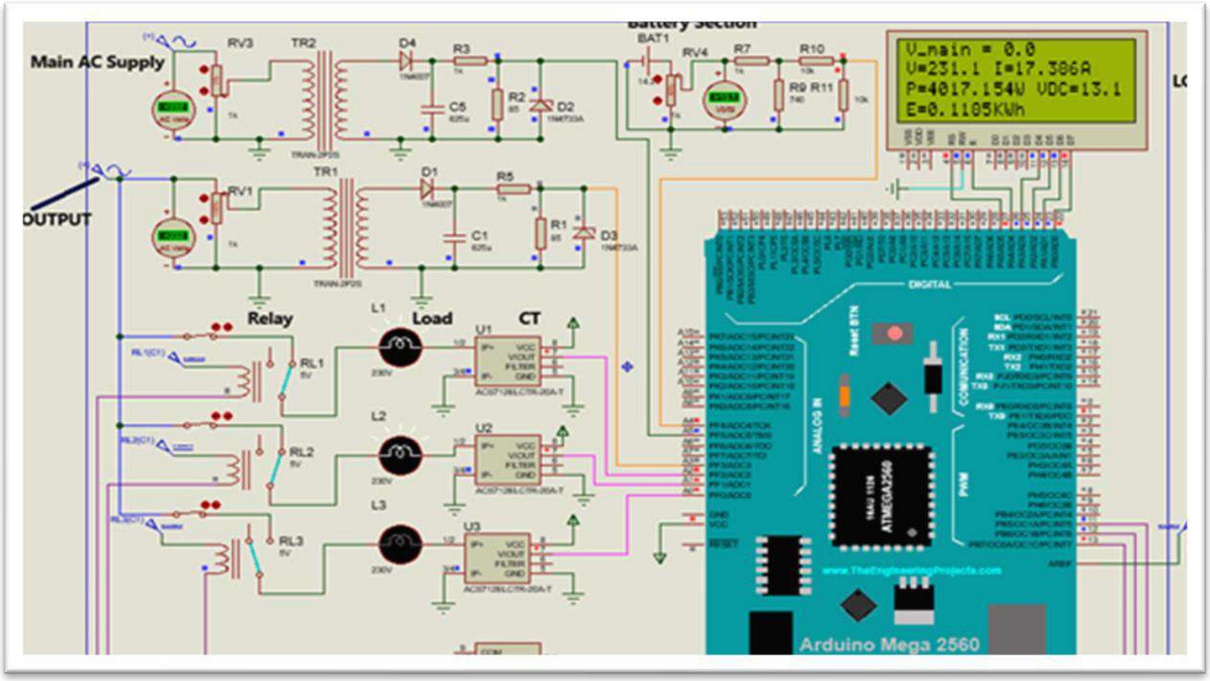

Figure 15: Load 3 connected Proteus schematics showing the interlinked circuit designs.

The guardrail "if S_SS>=aSmax then toss lowest-priority active circuit" empirically verifies the elimination of incipient overloads at the circuit level with a single human-readable control action, which the authors propose in the literature review as a priority-aware control rationale (where priority serves as a user utility proxy and a first-class decision variable). The recovery of service whenever headroom occurs, as shown in the battery-recovery cases, demonstrates that the two-time constant design (fast protective followed by slow restorative) is effective under both steady-state and step-change conditions.

The proposed system conducts a systematic investigation of battery-aware strategies through a tiered thresholding approach with three distinct stages, utilizing the measured DC bus voltage as a practical proxy for the actual battery state. This proxy metric enables the controller to make real-time decisions on prioritization and selective load shedding, aiming to optimize system resilience during periods of energy unavailability. In particular, when the sensing battery voltage drops below the critical threshold value of 11.4 V, experimentally found to be the first alarm level, an automatic shedding request is issued by the controller. At this point, the circuit at the lowest point of the hierarchy is purposely removed. The justification for this decision is that the energy storage system still has capacity available for the circuits and subsystems of higher priority, which are more important from an operational continuity standpoint. The decoupling event has a measurable and instantaneous impact on the composite system performance measure, SSo, which is the cumulative contribution of all subsystems connected. Specifically, a sharp downward step in Sss, when a circuit of the lowest priority is removed, indicates the loss of the circuit's share of the total system service. However, the shedding strategy achieves the goal of ensuring the uninterrupted operation of the highest-priority load P1, whose uptime is maintained even under degrading supply conditions. This result confirms the quality of the staged threshold approach, where the sacrifice of less critical elements leads to the prevention of catastrophic failure at all tiers. Figure 16 is a graphical representation of this chain of events, showing both the voltage-controlled trigger point and the system's response. As can be seen in the figure, the controller reacts instantly when the

DC bus falls below a predetermined value of 11.4 V, resulting in a discontinuous reduction of S_ss. At the same time, the performance of P1 remains unaffected. The hierarchical load management mechanism illustrated here is fundamental in achieving higher operational availability when the energy supply is limited and the load demand exceeds the available energy supply at any given time.

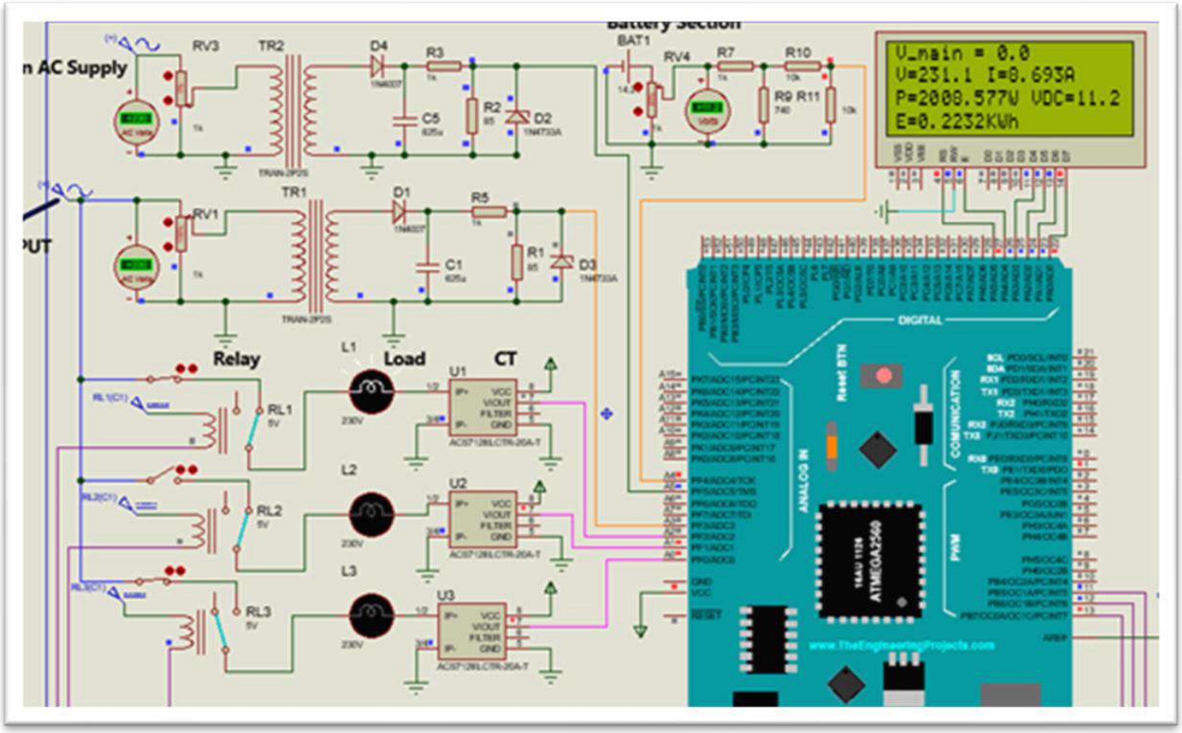

Figure 16: Proteus schematic system response when the battery voltage drops below the 11.4 V

If discharge continues and the battery falls below 11.0 V, the policy retains only the highest-priority circuit as shown in Figure 17; this setting effectively imposes a "lifeboat" configuration designed to extend autonomy for the single most critical branch.

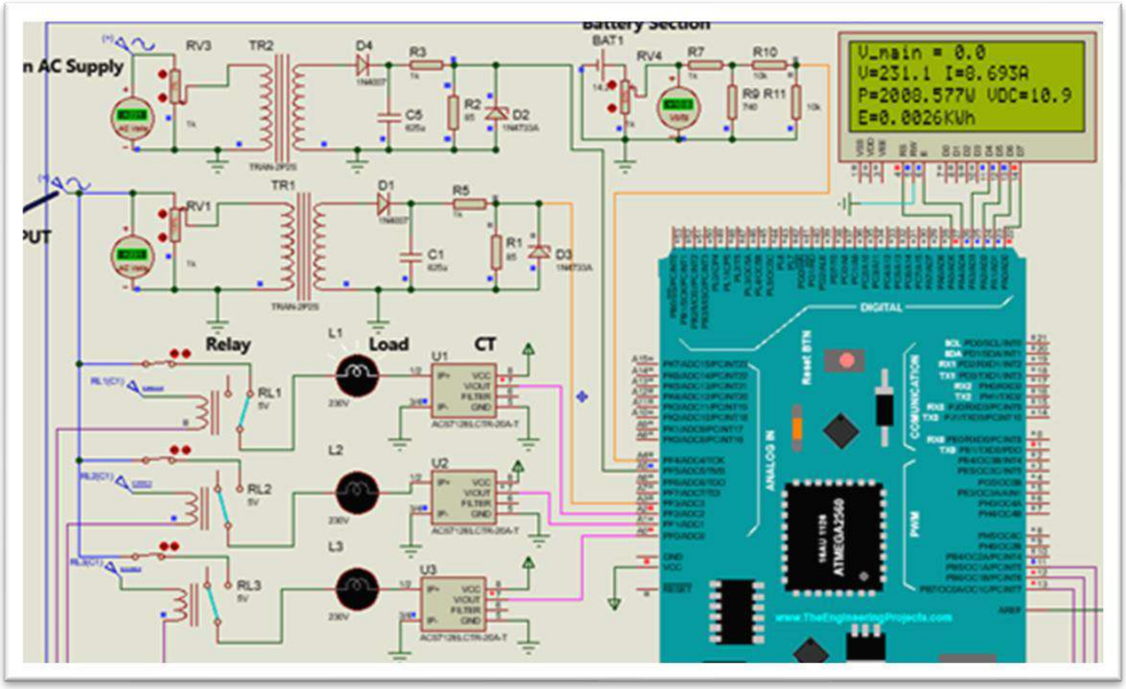

Figure 17: Proteus schematic system response when the battery voltage drops below 11 V

Finally, when the battery voltage is less than the critical voltage of 10.5 volts, the controller will carry out a complete shutdown process, disconnecting all related loads. This is a deliberate action to prevent deep discharge and thereby reduce the possibility of irreparable damage, reduced capacity, or a shorter operational life to the energy storage system. At this point, the system also issues a protective alert by displaying a warning text on the liquid-crystal display, providing the user with clear and immediate information on the shutdown event and its underlying cause, as shown in Figure 18. This provision ensures that the person responsible for this operation not only knows that there is an interruption but that it is a safeguarded response to ensure the safety of the energy source.

The integration of this ultimate cutoff and the antecedent thresholds establishes a structured, three-tiered load management structure. Collectively, all these bands provide for a stepwise and monotonic decrease of load in proportion to progressive depletion of the available drop reserve. Systematically shutting down circuits in accordance with their assigned priority, the system maintains the operational continuity of the most critical system functions for as long as possible before executing the final shutdown. This approach strikes a conscious balance between the availability of service and the protection of the battery.

Equally important is the demonstration of reversibility in the decision-making process. After the voltage level is restored, either due to a reduction in load or the restoration of the mains supply, the controller does not simply reconnect all the circuits at once. Instead, it gradually re-admits loads, starting with the circuit with the highest priority and re-admits them in the order from highest to lowest.

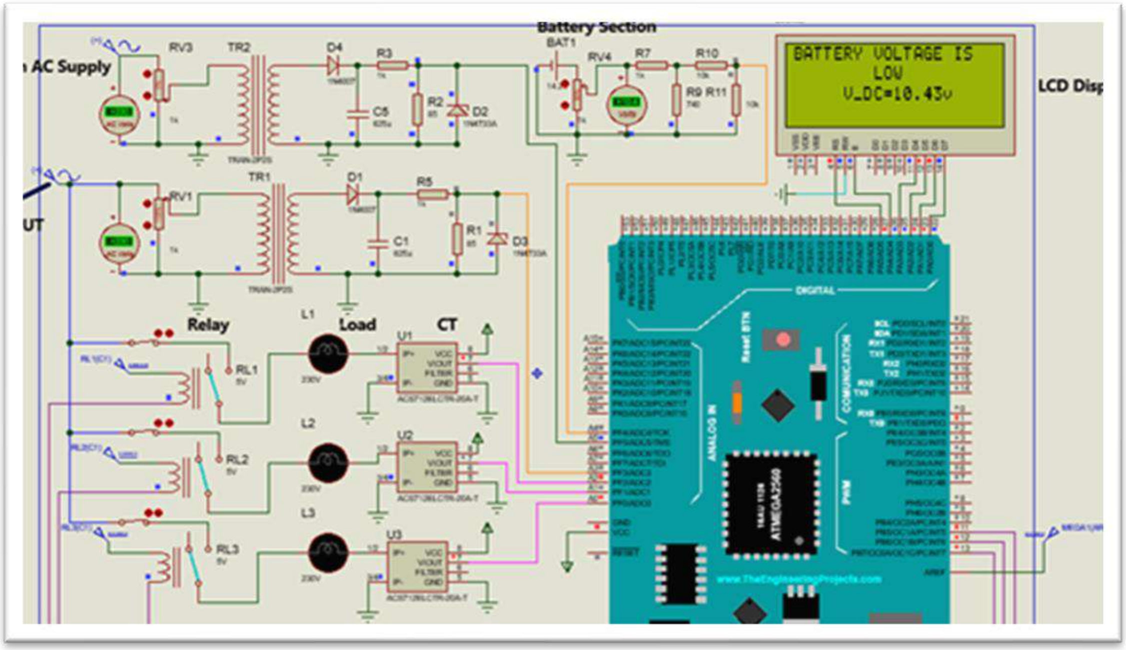

Figure 18: Proteus schematic system response when the battery voltage drops below 10.5 V

The restoration of the circuit paths only occurs in cases where there is still sufficient voltage headroom, which ensures system stability is maintained. By strictly enforcing these requirements, the design preempts the potential for oscillations in the system, such as relay chatter and rapid cyclic load connection/disconnection, which could hurt both user experience and hardware lifespan.

DISCUSSION:

The present investigation yields two main observations that place the empirical results within the methodological framework introduced in the preceding framework. The first observation is related to the deliberate decision to operate at the circuit level while attaching explicit priority tags. This architectural decision facilitates the representation of user intent by reducing it to a concise and robust control schema. Rather than endeavouring to model or forecast the behaviour of individual appliances—an endeavour that would require exhaustive analysis of schedules, as well as predictive modelling—the controller views each circuit as an entity endowed with a predetermined importance level. The step of the overload test is evidence of the effectiveness of this abstraction beyond any doubt. In view of the branch ratings and the singular aggregate capacity ceiling defined in the previous sections, the controller successfully restores the system's operational feasibility through the least invasive corrective maneuver: detaching the least important active branch. This action, targeted at stabilizing the system without provoking widespread disconnects or requiring complex predictive logic, provides evidence for the practicality of the method.

methodology

The second is that of the staged voltage thresholds, which are the basis of battery-aware logic. These thresholds provide a natural and straightforward mapping between the system's state and the corresponding control action, allowing humans to understand and explain the controller's actions easily. When the power reaches 11.4 volts, the system initiates a process known as "trim," shedding unnecessary loads. At eleven volts, the system enters "keep-only-essentials" mode, where it maintains only the highest-priority branches. Finally, at 10.5 volts,

the system performs a complete protective shutdown, disconnecting all loads to protect the battery. Meanwhile, a warning message is displayed on the LCD interface to inform the user of the termination. Although the current simulation uses voltage as a proxy for battery state of charge, the controller behaviour observed is consistent with arguments advanced during the literature review: autonomy-aware decisions, preferably enforced by lightweight estimators of state of charge and health, can improve the quality of load shedding and the reliability of restoration, and, as a result, prolong the asset life.
The transfer scenarios further demonstrate how this logic changes in response to a change in the source of supply. Under regular mains presence, all user-enabled circuits within their branch ratings are admitted without restriction. The inverted UPS source immediately assumes the role of source when the mains is lost, and this capacity-enhancement and priority-shedding logic will continue to be enforced without the need for manual reconfiguration. From a resiliency standpoint, this behavior reflects the principles of the well-known "fast shed, slow restore" pattern of microgrid protection strategy: a fast-acting protective response to an adverse event followed by cautious, priority-based restoration after re-establishing the system constraints. This consistency suggests that hierarchical control represents an appropriate guiding abstraction.
In all cases, the LCD interface played a key role in keeping operators informed. It provided a good visualization of the current system state, the threshold values, and the actions taken, both at the admission of new loads and at shedding events. However, results are also presented that suggest difficulties in the relay- and threshold-driven nature of the control policy. Prior work summarized in the thesis has warned that electromechanical relays may exhibit a degree of hysteresis in their activation and deactivation voltages that is not necessarily exactly in line with their nominal coil ratings. If no kind of braking mechanism is designed, a system is likely to vibrate at marginal voltage conditions, causing nuisance cycling or "chatter." Although the simulation results presented here have stabilized reconnection, any physical hardware implementation should include explicit timing delays as well as firmware-based mechanisms to ensure stability during

The experimental results also highlight the importance of correctly measuring channels, which has been established within the methodology. Branch currents are taken from current transformer channels, and voltages are measured from a potential transformer front end. The accuracy of the admission and shedding logic is essentially the product of the measurement reproducibility and linearity of each of these sensing channels over the ranges of operation in which they are used. A future hardware study should therefore repeat the validation process described elsewhere in the thesis, comparing the readings of the sensors against reference-grade instruments such as voltmeters, wattmeters, or clamp meters, in order to quantify the level of accuracy and to identify bias, in order to ensure that the performance of the hardware is the same as the level observed in simulation.
When the traces are viewed qualitatively, three recurring themes in performance can be identified. First, uptime is always maintained for critical loads for any outage sequence. The low-priority branch is always the first to experience capacity stress (Load 3 admission) or energy stress (battery decline), and the highest-priority branch will never reach this point until it is finally under the protective cutoff at 10.5 volts. Second, overload prevention is proactive rather than reactive: the moment the aggregate demand exceeds the ceiling, the controller takes one well-thought-out action to maximally restore feasibility and prevent cascading trips or incompetence, which is immediately demonstrated on the Load 3 admission test. Third, the restoration process demonstrates stability and consistency: loads are reconnected in a strictly prioritized order, i.e., the reconnection of each load is only allowed after it has been verified that there is adequate headroom to do so. Additionally, the simulation traces demonstrate clean and non-oscillatory re-energization of the circuits, even when transitioning out of deep-discharge protection and returning to regular operation.

Taken together, these findings validate that the system is consistent with the intent discussed in the chapter's discussion portion. The system performed as expected, reliably measuring metrics in real-time and responding appropriately to both low-battery and high-load stress, while protecting user-defined priorities and the UPS and connected equipment. From a methodological point of view, the choice to test the design in Proteus before the hardware version has been fruitful. The figure set displays all of the system's operating regimes: regular— mains supply, islanded operation with step increases in demand, and staged battery depletion—and records a coherent sequence of sensing, decision-making, and actuation.

CONCLUSION

The current investigation demonstrates that applying circuit-level priority constraints within a two-timescale policy is a reliable method for converting typical uninterruptible power supply (UPS) configurations from experiencing total power loss to achieving selective continuity. Overload Tripping is Preemptive. Aggregate Demand above the pre-determined Ceiling Is Uptime of the Highest-Priority Branch Is Maintained in Both Outage and Depletion Scenarios, And Restoration Follows a Strict Priority Sequence, Yielding Clean and Non-Oscillatory Dynamics.

The simulation model uses the terminal voltage bands as a pragmatic representation of reserve capacity. However, both the results of the analysis in the manuscript and the mentioned literature suggest the need for combining lightweight State-of-Charge (SoC) and State-of-Health (SoH) estimation, which can be obtained from data-driven or neural network methods, to determine the hysteretic bands. The controller architecture is specifically designed to receive estimates from a battery management system (BMS) or external estimator and then apply the same priority logic. Moreover, the broader literature has explored strategies that utilize machine learning to assist in similar load shedding and restoration issues, highlighting that the distinction between fast protection and slower, context-aware recovery for restarting systems lends itself to model-analogous or data-driven improvements.

Combined with the existing measurement channels and local telemetry, this rule-based prototype serves as a transparent benchmark and data channel, enabling the incremental integration of machine learning or artificial intelligence techniques. Such integration combines to improve reserve awareness, admission making, and restoration timing while maintaining the operational explainability and circuit-granularity of control to which the current actuation scheme is subject.

REFERENCES

[1] Riello UPS, "What Is Load Shedding and How Can It Extend UPS Battery Runtime?," FAQs, 2025. Available: https://www.riello-ups.com/questions/40-what-is-load-shedding-and-how-can-it-extend-ups-battery-runtime

[2] Leviton, "They Modern Load Center – The Most Modular Smart Home Solution", product page, 2025. Available: https://leviton.com/products/residential/load-centers/the-leviton-smart-load-center

[3] SPAN, "SPAN® Panel," product page, 2025. Available: https://www.span.io/panel

[4] L. McCabe, "Smart panels: what you need to know," *EnergySage*, updated Apr. 30, 2024. Available: https://www.energysage.com/energy-management/smart-panels/

[5] J. Yang, Q. Sun, L. Yao, Y. Liu, T. Yang, C. Chu, L. Fang, and L. Zhu, "A novel dynamic load-priority-based scheduling strategy for home energy management system," J. Cleaner Prod., vol. 389, p. 135978, Feb. 2023, doi: 10.1016/j.jclepro.2023.135978.

[6] S. Panda, I. S. Samanta, P. K. Rout, B. K. Sahu, M. Bajaj, V. Blázek, L. Prokop, and S. Mišák, "Priority-based scheduling in residential energy management systems integrated with renewable sources using adaptive Salp Swarm algorithm," Results Eng., vol. 23, p. 102643, Sept. 2024, doi: 10.1016/j.rineng.2024.102643.

[7] D. Kanakadhurga and N. Prabaharan, "Smart home energy management using demand response with uncertainty analysis of electric vehicle in the presence of renewable energy sources," Appl. Energy, vol. 364, p. 123062, Apr. 2024, doi: 10.1016/j.apenergy.2024.123062.

[8] H. Apaydin-Özkan, "An appliance scheduling system for residential energy management," *Sensors*, vol. 21, no. 9, art. no. 3287, May 10, 2021, doi: 10.3390/s21093287.

[9] C. Wang, Z. Wang, S. Chu, H. Ma, N. Yang, Z. Zhao, C. S. Lai, and L. L. Lai, "A two-stage under-frequency load-shedding strategy for microgrid groups considering risk avoidance," Appl. Energy, vol. 367, p. 123343, Aug. 2024, doi: 10.1016/j.apenergy.2024.123343.

[10] T. Skrjanc, R. Mihalič, and U. Rudež, "A systematic literature review on under-frequency load shedding protection using clustering methods," Renewable and Sustainable Energy Reviews, vol. 180, p. 113294, Jul. 2023, doi: 10.1016/j.rser.2023.113294.

[11] M. Uddin, H. Mo, D. Dong, S. Elsawah, J. Zhu, and J. M. Guerrero, "Microgrids: A review, outstanding issues and future trends," *Energy Strategy Reviews*, vol. 49, art. no. 101127, Sept. 2023, doi: 10.1016/j.esr.2023.101127.

[12] P. C. Bolsi, E. O. Prado, A. C. C. Lima, H. C. Sartori, and J. R. Pinheiro, "Battery autonomy estimation method applied to lead–acid batteries in uninterruptible power supplies," Journal of Energy Storage, vol. 58, p. 106421, Jan. 2023, doi: 10.1016/j.est.2022.106421.

[13] Y. Shang, W. Zheng, X. Yan, D. H. Nguyen, and L. Jian, "Predicting the state of health of VRLA batteries in UPS using data-driven method," Energy Rep., vol. 9, pp. 184–190, Sep. 2023, doi: 10.1016/j.egyr.2023.04.264.

[14] Y. Fan, Q. Lin, and R. Huang, "Non-invasive method-based estimation of battery state-of-health with dynamical response characteristics of load surges," Energies, vol. 17, no. 3, p. 583, 2024, doi: 10.3390/en17030583.

[15] M. O. Oloyede, G. A. Akpakwu, H. C. Myburgh, A. De Freitas, and T. Kunatsa, "A review on state-of-charge estimation methods, energy storage technologies and state-of-the-art simulators: Recent developments and challenges," *World Electric Vehicle Journal*, vol. 15, no. 9, art. no. 381, 2024, doi: 10.3390/wevj15090381.

[16] M. Havrlík, M. Libra, V. Poulek, and P. Kouřím, "Analysis of output signal distortion of galvanic-isolation circuits for monitoring the mains voltage waveform," Sensors, vol. 22, no. 20, p. 7769, 2022, doi: 10.3390/s22207769.

[17] C. Tang, J. Liang, Q. Zhu, X. Lu, J. Shu, and C. Jiang, "Review of the current transducer techniques," Discover Applied Sciences, vol. 6, p. 351, 2024, doi: 10.1007/s42452-024-06059-x.

[18] H.-L. Tsai, L. P. Truong, and W.-H. Hsieh, "Design and evaluation of a wireless power-monitoring IoT system for AC appliances," Energies, vol. 16, no. 1, p. 163, 2023, doi: 10.3390/en16010163.

[19] P. Alqinsi, N. Ismail, I. J. M. Edward, and W. Darmalaksana, "IoT-based UPS monitoring system using MQTT protocols," in Proc. 4th Int. Conf. Wireless and Telematics (ICWT), 2018, pp. 1–5, doi: 10.1109/ICWT.2018.8527815.

[20] J. A. J. Shirley, H. Manivelan, P. Khare and M. J. B. Reddy, "Dynamic load shedding and system restoration using wide area measurements," IET Generation, Transmission and Distribution, vol. 18, no. 17, pp. 2860–2874, 2024, doi: 10.1049/gtd2.13240.

[21] N. Ramachandra and R. Natarajan, "State-of-the-art and real-time implementation of an IoT-enabled energy management system for a cluster of dwellings," Heliyon, vol. 10, no. 16, 2024, doi: 10.1016/j.heliyon.2024.e35887.

[22] Leviton Manufacturing Co., Inc., *The Smart Leviton Load Center: Single Panel Solution for Managing Essential and Nonessential Circuits with a Generator* [User Guide]. Leviton, 2023. Available:https://leviton.com/content/dam/leviton/residential/product_documents/user_guide-manual/Leviton-ATS-integration-for-essential-circuits-guide.pdf